Congreso Nacional de Control Automático 2013
Ensenada, Baja California, Mexico, Octubre 16-18, 2013

Adaptive Backstepping Controller for Internal Combustion Engine with Actuator Dynamics

Marco Meza-Aguilar,[1] Antonio Navarrete-Guzmán,[1] Alexander Loukianov[1] and Jorge Rivera[2]
[1] Department of Electrical Engineering
CINVESTAV Unidad Guadalajara, 45019, Zapopan, Jalisco, México
[2] Department of Electronic Engineering
DIVEC CUCEI, University of Guadalajara, 44430, Guadalajara, Jalisco, México
mail:ameza@gdl.cinvestav.mx, anavarret@gdl.cinvestav.mx, louk@gdl.cinvestav.mx, jorge.rivera@cucei.udg.mx

Abstract— **In this work, it is presented a control law for an internal combustion engine that takes into account the actuator dynamics. The internal combustion engine is controlled by means of an adaptive backstepping algorithm. Then, the control input signal to the engine (throttle angle) is used as a reference signal for the actuator which is driven by a direct current motor. A higher-order sliding mode controller is applied to the actuator in order that it can track the control input signal for finally regulating the velocity of the combustion engine.**
keywords: sliding modes, adaptive backstepping, internal combustion engine.

I. Introduction

The automotive industry is constantly pursuing to satisfy the end-user demand of fuel efficient engines along with free running of the vehicle. Moreover, almost every modern car is equipped with on-board diagnostic software in their electronic control units (ECUs) to control and monitor the engine operations.

Therefore several researchers are focusing in solving the problem of designing feedback controllers for the major subsystem of a vehicle that enables further improvement via application of modern speed control strategies in a combustion engine with an electrically driven throttle.

The engine speed control problem has been considered in several publications (Moskwa and Hedrick, 1987), (Guzzella and Onder, 2010), (Ahmed and Bhatti, 2010). Usually, these controllers are based on mean value engine models (MVEMs) (Hendricks and Sorenson, 1990*b*) because it can describe the behavior of spark ignition (SI) engines (Hendricks and Vesterholm, 1992), (Hendricks and Sorenson, 1990*a*). The MVEMs models describe the time development of the most important measurable engine variables (or states) on time scales larger that an engine cycle (Hendricks, 1989), (Rajamani, 2012). The states of an SI engine are usually the fuel film flow or mass, the crank shaft speed and manifold pressure, each described with differential equations driven by control inputs such as the injected fuel flow, spark advance and throttle angle, respectively.

The sliding modes (SM) technique has been widely discussed and used in large number of works. This algorithm exhibits high gain and provides to the closed-loop system some invariance properties such as external disturbance rejection and robustness to plant parametric variations, and, moreover, the order reduction (Drakunov and Utkin, 1992), (Utkin, 1993). Due to these advantages and simplicity of the methodology, this technique is largely implemented to solve various control problems. The application of the SM in the automotive area has taken much importance, (Loukianov *et al.*, 1997), (Shraim *et al.*, 2008), (Imine *et al.*, 2011), (Delprat and Ferreira de Loza, 2012), due to the characteristics that present SM algorithm.

In this work, a novel control scheme is presented to regulate the speed of a combustion engine driven by a direct current (DC) motor that acts as an actuator. The controller design is based on adaptive backstepping approach (Krstic *et al.*, 1995) combined with high-order SM (HOSM) algorithms (Levant., 2003). The particular structure of MVEMs allows the adaptive backstepping control technique to be applied in order to calculate the virtual control input signal to the engine (throttle angle). This signal is used as a reference signal for the actuator to formulate an adaptive sliding manifold. Then, the HOSM algorithm is applied to the actuator in order to achieve finite time convergence of the closed-loop system state vector to the designed sliding manifold, and regulate the throttle position of the combustion engine. As result, the engine speed tracking error asymptotically tends to zero.

The remaining of this work is organized as follows. In Section II, the mathematical models of MVEMs and DC actuator are presented. Section III establishes the control design to be tackled as the proposed solution to the considered problem. A simulation study is carried on in Section IV, and finally some comments conclude the work in Section V.

II. Mean Value Engine Models

In this section the mathematical model of the Mean Value Engine Model (MVEM) of Spark Ignition (SI) is presented (Hendricks and Luther, 2001).

II-A. The crank shaft speed

The crank shaft state equation is derived using straight forward energy conservation considerations. Energy is inserted into the crank shaft via the fuel flow. In order to avoid modeling the cooling and exhaust system losses, the thermal efficiency of the engine is inserted as a multiplier of the fuel mass flow. Losses in pumping and friction dissipate rotational energy while some of the energy goes into the load. Physically this is expressed as a conservation law: the rate of a change of the crank shaft rotational kinetic energy is equal to sum of the power available to accelerate the crank shaft and that of the load:

$$\dot{n}_e = -\frac{(P_f + P_p + P_b)}{J_e n_e} + \frac{H_u \eta_i \dot{m}_f}{J_e n_e} \tag{1}$$

where n_e is the crank shaft speed, J_e is the moment of inertia in the rotating parts of the engine, P_f, P_p and P_b are the power lost to the friction, pumping losses and the load, respectively, H_u is the fuel burn value, η_i is the thermal efficiency, and $\dot{m}_f$ is the fuel mass flow.
The loss functions P_f and P_p form the load input to the engine and can be implemented to match a desired operating scenario. They are usually regressions based on data from engine measurements and can be modeled by the following regressions functions:

$$\begin{aligned} P_f &= 0{,}0135 n_e^3 + 0{,}2720 n_e^2 + 1{,}6730 n_e \\ P_p &= n_e P_m (0{,}2060 n_e - 0{,}9690). \end{aligned} \tag{2}$$

where P_m is the pressure in the intake manifold. It has been found convenient to express the load power as the function:

$$P_b = k_b n_e^3 \tag{3}$$

where k_b is the loading parameter. It is ajusted in such a way than the engine is loaded to the desired power or torque level at a given operating point.

The thermal efficiency η_i is also a regression and can be modeled by the following polynomial:

$$\eta_i = 0{,}55(1 - 0{,}39 {n_e}^{-0{,}36})(0{,}82 + 0{,}52 P_m - 0{,}39 {P_m}^2). \tag{4}$$

II-B. The fuel mass flow rate

The fuel mass flow rate $\dot{m}_f$ is typically determined by a fuel injection control system which attempts to maintain a stoichiometric air fuel ratio. It is assumed this ratio is successfully maintained in the cylinder. Thus, the fuel mass flow rate $\dot{m}_f$ is related to the outflow from the intake manifold into the cylinders of the engine as follows (Rajamani, 2012):

$$\dot{m}_f = \frac{\dot{m}_{ao}}{\lambda L_{th}} \tag{5}$$

where $\dot{m}_{ao}$ is the air mass flow rate out of the intake manifold and into the cylinder, L_{th} is the stoichiometric air/fuel mass ratio for the Fuel and λ is the air/fuel equivalence ratio.

II-C. Manifold Pressure Equation

In the derivation of the manifold pressure state equation the common procedure is to use the conservation of air mass in the intake manifold:

$$\dot{m}_m = \dot{m}_{ai} - \dot{m}_{ao} \tag{6}$$

where $\dot{m}_m$ is the air mass flow in the intake manifold, $\dot{m}_{ai}$ and $\dot{m}_{ao}$ represent mass flow rate in and out of the intake manifold i.e. through the throttle valve and into the cylinder respectively.
The pressure in the intake manifold P_m can be related to the air mass in the manifold m_m using the ideal gas equation

$$P_m V_m = m_m R T_m \tag{7}$$

where R is the ideal gas constant, T_m is the intake manifold temperature and V_m is the intake manifold volume.
Taking time derivates of (7) and using (6), the intake manifold pressure equation is obtained of the form

$$\dot{P}_m = \frac{R T_m}{V_m}(\dot{m}_{ai} - \dot{m}_{ao}). \tag{8}$$

The expressions forms of $\dot{m}_{ai}$ and $\dot{m}_{ao}$ are described in the following Subsections.

II-C.1. Port air mass flow: The air mass flow at the intake port of the engine, can be obtained from the speed-density equation (Hendricks and Luther, 2001) as

$$\dot{m}_{ao} = \sqrt{\frac{T_m}{T_a}} \frac{V_d}{120 R T_m} (e_v P_m) n_e. \tag{9}$$

the volumetric efficiency e_v can be described by the following simple equation taken from (Hendricks *et al.*, 1996)

$$e_v P_m = s_i P_m - y_i \tag{10}$$

where T_a is the ambient temperature, V_d is the engine displacement, the manifold pressure slope s_i is slightly less than 1 and the manifold pressure intercept y_i is close to $0{,}10$; they are always positive and depend mostly on the crank shaft speed. Moreover, they should not change much over the range operating from one engine to another except for those which are highly tuned. The form of equation (10) has been known phenomenologically at Ford for many years but in (Hendricks *et al.*, 1996) this equation has been derived from physical considerations. This means that it can be rapidly applied to many different engines with basically only a knowledge of a few physical constants and this is the advantage of the derivation above.

Using now (10) the speed-density equation (9) becomes

$$\dot{m}_{ao} = \sqrt{\frac{T_m}{T_a}} \frac{V_d}{120 R T_m} (s_i P_m + y_i) n_e. \tag{11}$$

II-C.2. Throttle air mass flow: The second important equation is the manifold pressure state equation which is used to describe the air mass flow past the throttle plate. This part of the model based on the isentropic flow equation for a converging-diverging nozzle, is given by (Hendricks and Luther, 2001)

$$\dot{m}_{ai} = \dot{m}_{ai1}\frac{P_a}{\sqrt{T_m}}\beta_1(\alpha)\beta_2(P_r) + \dot{m}_{ai0} \tag{12}$$

where P_a is the ambient pressure, $\dot{m}_{ai1}$ and $\dot{m}_{ai0}$ are constants, α is the throttle angle and $\beta_1(\alpha)$ is the throttle plate angle dependency which can be described by the following function as an approximation to the normalized open area:

$$\beta_1(\alpha) = 1 - \cos(\alpha) - \frac{{\alpha_0}^2}{2} \tag{13}$$

where α_0 is the fully closed throttle plate angle (radians).

The function $\beta_1(\alpha)$ serves as the function of an area dependent discharge coefficient and $\beta_2(P_r)$ is the isentropic flow expression:

$$\beta_2(P_r) = \begin{cases} 1 & P_r < P_c \\ \sqrt{1 - \left(\frac{P_r - P_c}{1 - P_c}\right)} & P_c \leq P_r \end{cases} \tag{14}$$

where $P_r = P_m/P_a$, and $P_c = 0{,}4125$ is the critical pressure (turbulent flow), and this function is differentiable to piecewise and there is not rapid commutation in the point switch.

II-D. Engine motor model

Using (1-14), the MVEMs state system is obtained of the following form:

$$\begin{aligned} \dot{n_e} &= -f_1(n_e, P_m) + b_1(n_e, P_m)P_m \\ \dot{P}_m &= \frac{RT_m}{V_m}\left(f_2(n, P_m) + b_2(P_m)\beta_1(\alpha)\right) \end{aligned} \tag{15}$$

where
$f_1(n_e, P_m) = \frac{P_f + P_p + P_b}{J_e n_e}$,
$b_1(n_e, P_m) = \left(\frac{H_u \eta_i \sqrt{T_m/T_a} V_d}{120 I R T_m \lambda L_{th}}\right)(\frac{y_i}{P_m} + s_i)$,
$f_2(n_e, P_m) = \dot{m_{ai0}} - \sqrt{\frac{T_m}{T_a}}\frac{V_d}{120 R T_m}(s_i P_m + y_i)n_e$,
$b_2(n_e, P_m) = \dot{m_{ai1}}\frac{P_a}{\sqrt{T_m}}\beta_2(P_r)$.

II-E. Actuator model

The DC drive dynamics (Gottlieb, 1994), possesses a block structure controllable (Loukianov, 1998):

$$\begin{aligned} \frac{d\alpha}{dt} &= \omega_a \\ \frac{d\omega_a}{dt} &= \frac{k_t i_a - T_L}{J} \\ \frac{di_a}{dt} &= \frac{-Ri_a - \lambda_0 \omega_a + \upsilon_a}{L} \end{aligned} \tag{16}$$

where α, ω_a, i_a and υ_a are the position, speed, current and voltage, respectively, of the throttle drive, T_L is the drive load torque, J is the moment of inertia, L and R are the drive inductance and resistance, respectively, and k_t and λ_0 are the torque and e.m.f. constants, respectively.

II-F. The complete model

A block diagram of the complete closed-loop system is shown in Fig 1. To satisfy the control objective, which is to

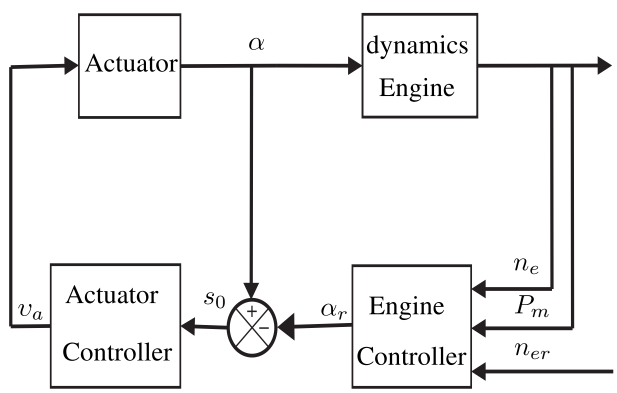

Fig. 1. Block diagram of closed-loop system

force the engine speed n_e to track some desired reference n_{er}, we define the control errors and new state variables as

$$x_1 = n_e - n_{er},\ x_2 = P_m,\ x_3 = \alpha,\ x_4 = \omega_a,\ x_5 = i_a$$

where n_{er} and α_r is the engine speed and throttle position reference, respectively. Then, using the engine model (15) and actuator model (16) the complete model system is presented of the form

$$\begin{aligned} \dot{x}_1 &= \bar{f}_1(x_1, \varphi) + \bar{b}_1(x_1, \varphi)x_2 \\ \dot{x}_2 &= \bar{f}_2(x_1, x_2) + \bar{b}_2(x_2)\beta_1(x_3) \\ \dot{x}_3 &= x_4 \\ \dot{x}_4 &= a_{45}x_5 - a_{40}T_L \\ \dot{x}_5 &= a_{55}x_5 - a_{54}x_4 + b_5\upsilon_a \end{aligned} \tag{17}$$

where
$\bar{f}_1(x_1, \varphi) = -\frac{P_f + P_b}{J_e(x_1 + n_{er})} + \dot{n}_{er} + \varphi y_i$,
$\bar{b}_1(x_1, \varphi) = -(\frac{P_p}{J_e(x_1 + n_{er})} - \varphi s_i)$,
$\varphi = \left(\frac{H_u \eta_i \sqrt{T_m/T_a} V_d}{120 J_e R T_m \lambda L_{th}}\right)$,
$\bar{f}_2(x_1, x_2) = \frac{RT_m}{V_m}(\dot{m_{ai0}} - \sqrt{\frac{T_m}{T_a}}\frac{V_d}{120 R T_m}(s_i x_2 + y_i)(x_1 + n_r))$,
$\bar{b}_2(x_2) = \frac{RT_m}{V_m}(\dot{m_{ai1}}\frac{P_a}{\sqrt{T_m}}\beta_2(x_2))$,
$a_{45} = \frac{k_t}{J}$, $a_{40} = \frac{1}{J}$, $a_{54} = \frac{\lambda_0}{L}$, $a_{55} = \frac{R}{L}$ and $b_5 = \frac{1}{L}$

Assumption H1. The function φ is constant on stable state, that means, its derivative on stable state is zero $\dot{\varphi} = 0$

III. Control design

In the control design, we consider the thermal efficiency η_i (4) as an unknown function of the state variables; that leads to an unknown value of the function φ in (17)

III-A. *Engine adaptive backstepping controller design*

Subsystem (17) has the strict feedback or block controllable form, and the relative degree of the system with respect to the tracking error x_1 is too high and equal to five. To solve this problem and estimate the unknown function φ, the combination of the adaptive backstepping technique (Krstic *et al.*, 1995) and high-order sliding modes algorithm (Levant., 2003) be will be implemented in order to design, first, an adaptive sliding manifold, and then the third order sliding mode algorithm will be implemented to make this manifold attractive. Defining $z_1 = x_1$, which is the output to be forced to zero and setting $\tilde{\varphi} = \varphi - \hat{\varphi}$, where $\hat{\varphi}$ is the estimate of φ, a Lyapunov function candidate is proposed as

$$V_1 = \frac{1}{2}(z_1^2 + \gamma_1^{-1}\tilde{\varphi}^2) \qquad (18)$$

where γ_1^{-1} is an adaptation gain. The time derivative of (18) along the trajectories of (17) under Assumption H1 is calculated of the form

$$\begin{aligned} \dot{V}_1 &= z_1\dot{z}_1 - \gamma_1^{-1}\tilde{\varphi}\dot{\hat{\varphi}} \\ &= z_1\left(\bar{f}_1(x_1,\hat{\varphi}) + \bar{b}_1(x_1,\hat{\varphi})x_2 + \tilde{\varphi}(y_i + s_i x_2)\right) \\ &- \gamma_1^{-1}\tilde{\varphi}\dot{\hat{\varphi}}. \end{aligned} \qquad (19)$$

The desired value x_{2r} of the virtual control x_2 in the first block of (17) is selected in order to introduce a desired dynamics $-k_1 z_1$:

$$x_{2r} = \frac{-k_1 z_1 - \bar{f}_1(x_1,\hat{\varphi})}{\bar{b}_1(x_1,\hat{\varphi})}. \qquad (20)$$

with $k_1 > 0$. Now, defining the second error

$$z_2 = x_2 - x_{2r}$$

and substituting (20) in (19) yields

$$\begin{aligned} \dot{V}_1 &= -k_1 z_1^2 + \bar{b}_1(x_1,\hat{\varphi})z_1 z_2 + \tilde{\varphi}(y_i + s_i x_2)z_1 \\ &- \gamma_1^{-1}\tilde{\varphi}_1\dot{\hat{\varphi}}_1 \\ &= -k_1 z_1^2 + \bar{b}_1(x_1,\hat{\varphi})z_1 z_2 \\ &+ \tilde{\varphi}_1((y_i + s_i x_2)z_1 - \gamma_1^{-1}\dot{\hat{\varphi}}_1). \end{aligned} \qquad (21)$$

Then, defining the tuning function

$$\tau_1 = (y_i + s_i x_2)z_1 \qquad (22)$$

the derivative (21) can be rewritten as follows:

$$\dot{V}_1 = -k_1 z_1^2 + \bar{b}_1(x_1,\hat{\varphi})z_1 z_2 + \tilde{\varphi}_1(\tau_1 - \gamma_1^{-1}\dot{\hat{\varphi}}_1). \qquad (23)$$

At the second step, it is formed the following Lyapunov function candidate:

$$V_2 = V_1 + \frac{1}{2}z_2^2. \qquad (24)$$

Taking the time derivative of (24) results in

$$\begin{aligned} \dot{V}_2 &= \dot{V}_1 + z_2\dot{z}_2 \\ &= \dot{V}_1 + z_2(\bar{f}_2(x_1,x_2) + \bar{b}_2(x_2)v(x_3) - \dot{x}_{2r}). \end{aligned} \qquad (25)$$

where $v(x_3) = \beta_1(x_3))$. To introduce the desired dynamics $-k_2 z_2$ for z_2, the desired value v_r of the virtual control $v(x_3)$ is proposed of the following form:

$$v_r = \frac{-k_2 z_2 - \bar{b}_1(x_1,\hat{\varphi})z_1 - \bar{f}_2(x_1,x_2) + \dot{x}_{2r}}{\bar{b}_2(x_2)} \qquad (26)$$

with $k_2 > 0$, where the derivative $\dot{x}_{2r}$ can be obtained by means of a robust exact differentiator proposed in (Levant., 2003).
Setting

$$z_3 = v(x_3) - v_r \qquad (27)$$

and using (26) in (25) yields

$$\begin{aligned} \dot{V}_2 &= -k_1 z_1^2 - k_2 z_2^2 + \rho\bar{b}_2(x_2)z_2 z_3 \\ &+ \tilde{\varphi}_1\left(\tau_1 - \gamma_1^{-1}\dot{\hat{\varphi}}_1\right). \end{aligned} \qquad (28)$$

To eliminate the term with $\tilde{\varphi}_1$ in (28) the update law can be determined through the following equation:

$$\dot{\hat{\varphi}}_1 = \gamma_1\tau_1 \qquad (29)$$

and the equation (28) is reduced to

$$\dot{V}_2 = -k_1 z_1^2 - k_2 z_2^2 + \bar{b}_2(x_2)z_2 z_3. \qquad (30)$$

To calculate angle reference x_{3r} we put $z_3 = 0$, that means $v(x_{3r}) = v_r$, and using the expression (13), we have

$$1 - \cos(x_{3r}) - \frac{{\alpha_0}^2}{2} = v_r \qquad (31)$$

Thus,the drive reference angle x_{3r} is calculated as

$$x_{3r} = cos^{-1}\left(1 - v_r(x_{3r}) - \frac{\alpha_0^2}{2}\right). \qquad (32)$$

Now the sliding function s_0 is formulated as

$$s_0 = x_3 - x_{3r}. \qquad (33)$$

Then defining the derivatives

$$\begin{aligned} s_1 &= \dot{s}_0 \\ s_2 &= \dot{s}_1 \end{aligned}$$

system (17) in the new variables can be represented of the form

$$\begin{cases} \dot{z}_1 &= -k_1 z_1 + \bar{b}_1(x_1,\hat{\varphi})z_2 \\ \dot{z}_2 &= -\bar{b}_1(x_1,\hat{\varphi})z_1 - k_2 z_2 + s_0 \end{cases} \qquad (34)$$

$$\begin{cases} \dot{s}_0 &= s_1 \\ \dot{s}_1 &= s_2 \\ \dot{s}_2 &= f_s(x_1,x_2,x_3,x_4,x_5) - b_2 u \end{cases} \qquad (35)$$

where f_s is a continuous function bounded in a admissible region Ω by

$$|f_s(x_1,x_2,x_3,x_4,x_5)| \leq \gamma_0 < \infty \qquad (36)$$

and $b_2(\cdot) = a_{45}b_5$.

III-B. Actuator HOSM controller design

To enforce sliding mode motion on $s_0 = 0$, $s_1 = 0$ and $s_2 = 0$, we apply the following third-order sliding mode algorithm (Levant., 2003):

$$u = -u_0 \text{sign}[\psi_{2,3}(s_0, s_1, s_2)] \tag{37}$$

$$\psi_{2,3}(s_0, s_1, s_2) = s_2 + \beta_2 \left(|s_1|^3 + |s_0|\right)^{1/6} \text{sign}\left(s_1 + \beta_1 |s_0|^{2/3} \text{sign}(s_0)\right) \tag{38}$$

where u_0, β_1, and β_2 are the control gains. In (Levant., 2003), it was shown that there exits a set of constants $u_0 > 0$, $\beta_1 > 0$ and $\beta_2 > 0$ such that the state vector of the closed-loop sub system (35) under the condition (36) converges in finite time to the third-order SM set

$$s_0 = 0, \quad s_1 = 0, \quad s_2 = 0. \tag{39}$$

On the manifold $s_0 = 0$ (33), we have $x_3 = x_{3r}$, and from (27), (31) and (32) it follows $v = v_r$ or $z_3 = 0$. The motion on the sliding manifold $s_0 = 0$ (33) or $z_3 = 0$ (27) defined by (34) constrained to

$$\begin{aligned} \dot{z}_1 &= -k_1 z_1 + \bar{b}_1(x_1, \hat{\varphi}) z_2 \\ \dot{z}_2 &= -\bar{b}_1(x_1, \hat{\varphi}) z_1 - k_2 z_2. \end{aligned} \tag{40}$$

And the Lyapunov function derivative $\dot{V}_2$ (30) reduces to

$$\dot{V}_2 = -k_1 z_1^2 - k_2 z_2^2 < 0. \tag{41}$$

If we select the control gains as $k_1 > 0$ and $k_2 > 0$, then the system (40) will be asymptotically stable, that is the control errors $z_1(t)$ and $z_2(t)$ tends to zero as $t \to \infty$.

The implementation of the proposed third-order SM controller (37) requires the calculation of the derivatives s_1 and s_2. To obtain these derivatives again, a sliding mode exact robust differentiator can be employed. We use the second-order robust exact differentiator defined by

$$\begin{aligned} \dot{\xi}_0 &= \mu_0 \qquad \mu_0 = -\delta_0 |\xi_0 - s_0|^{2/3} \text{sign}(\xi_0 - s_0) + \xi_1 \\ \dot{\xi}_1 &= \mu_1 \qquad \mu_1 = -\delta_1 |\xi_1 - \mu_0|^{1/2} \text{sign}(\xi_1 - \mu_0) + \xi_2 \\ \dot{\xi}_2 &= -\delta_2 \text{sign}(\xi_2 - \mu_1) \end{aligned} \tag{42}$$

where ξ_0, ξ_1 and ξ_2 are the estimates of the sliding variable s_0 and its derivatives s_1 and s_2, respectively. In (Levant., 2003), it was shown that there exists $\delta_i > 0$, $i = 0, 1, 2$, such that the estimates ξ_0, ξ_1 and ξ_2 converge to the real variables s_0, s_1 and s_2, respectively, in finite time. These estimates are then implemented in controller (37) instead of the real variables.

IV. Simulations

In this section we verify the performance of the proposed control scheme by means of numeric simulations.

We considerer a MVEMs with the following nominal parameters (Hendricks *et al.*, 1996): $V_d = 1{,}275\ L$, $R = 0{,}00287$, $V_m = 0{,}0017$, $I = 480(2\pi/60)^2$, $H_u = 4300$, $L_{th} = 14{,}67$, $\lambda = 1{,}0$, $T_m = 293$, $T_a = 293$, $P_c = 0{,}4125$, $P_a = 1{,}013$, $P_r = P_m/P_a$, $\dot{m}_{ai1} = 5{,}9403$, $\dot{m}_{ai0} = 0$, $si = 0{,}961$, $yi = -0{,}07$. The velocity reference signal increases from 0,66 to 3 krpm in the first 8 s and then, it remains constant at 3 krpm $\in (8, 15]$ s, again increases from 3 krpm to 4 krpm $\in [15, 20]$ s, and finally remains constant in 4 krpm $\in [20, 30]$ s. The velocity of engine is shown in figure 2, where can be appreciated a good tracking performance with adapted parameters present in the controller. The tracking of the throttle position is presented in figure 3, we observe the acceptable performance that present this signal. And finally in the figure 4 the pressure generated for the engine is shown, similar to the before figures this has a good performance.

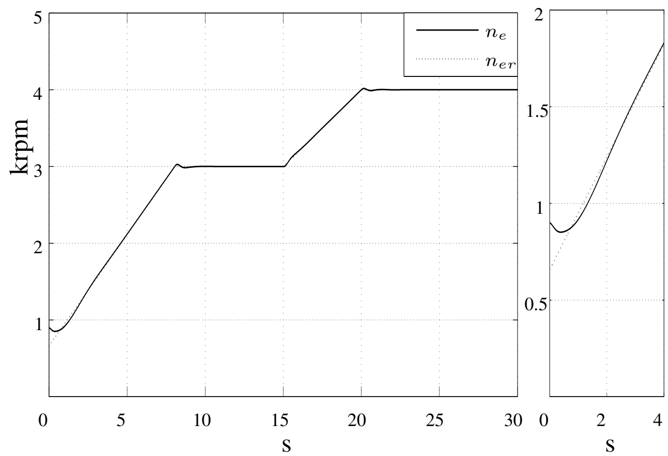

Fig. 2. Output velocity engine velocity

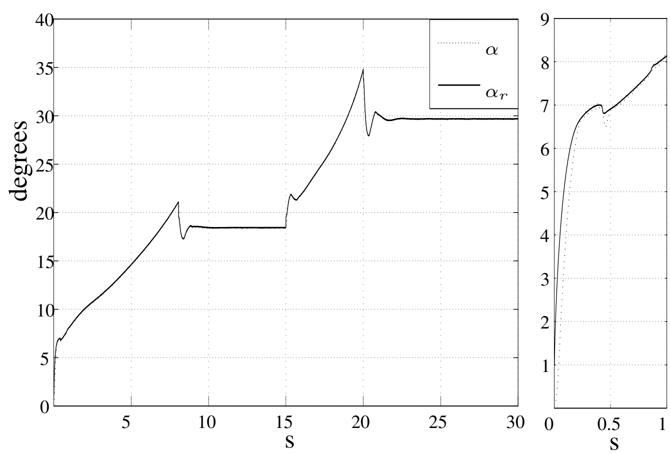

Fig. 3. Output tracking α position

V. Conclusions

In this work a controller for internal combustion engine is designed in the presence of the known thermal efficiency. The control design is based on a combination of the

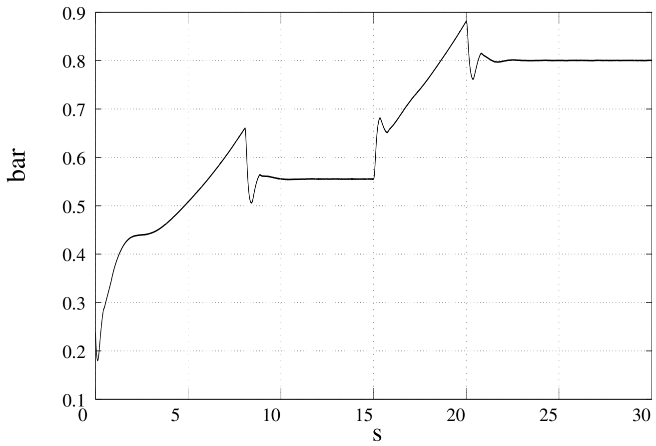

Fig. 4. Pressure in the manifold

adaptive backstepping and sliding mode control techniques. The adaptive backstepping is used to generate the adaptive sliding manifold on which the engine tracking error asymptotically tends to zero. The high-order sliding mode algorithm achieves the designed manifold be finite-time attractive. This fact is verified by numerical simulations.

REFERENCES

Ahmed, Q. and A.I. Bhatti (2010). Second order sliding mode observer for estimation of si engine volumetric efficiency amp; throttle discharge coefficient. In: *Variable Structure Systems (VSS), 2010 11th International Workshop on*. pp. 307 –312.

Delprat, S and A Ferreira de Loza (2012). High order sliding mode control for hybrid vehicle stability. *International Journal of Systems Science* (ahead-of-print), 1–11.

Drakunov, S. V. and V. I. Utkin (1992). Sliding mode control in dynamic systems. *International Journal of Control* **55**, 1029–1037.

Gottlieb, I. (1994). *Electric Motors and Control Techniques*. McGraw-Hill Education.

Guzzella, Lino and Christopher Onder (2010). *Introduction to Modeling and Control of Internal Combustion Engine Systems*. Springer.

Hendricks, Elbert (1989). Mean value modelling of large turbocharged two-stroke diesel engine. In: *SAE Technical Paper*. number 890564.

Hendricks, Elbert, Alain Chevalier, Michael Jensen, Spencer C. Sorenson, Dave Trumpy and Joe Asik (1996). Modelling of the intake manifold filling dynamics. In: *SAE Technical Paper*. number 960037.

Hendricks, Elbert and Jim Benjamin Luther (2001). Model and observer based control of internal combustion engines. In: *Proc. of the 1st Int. Workshop on Modeling Emissions and Control in Automotive Engines (MECA), Salerno, Italy*. pp. 9–20.

Hendricks, Elbert and Spencer C Sorenson (1990*a*). Mean value modelling of spark ignition engines. In: *SAE Technical Paper*. number 900616.

Hendricks, Elbert and Spencer Sorenson (1990*b*). Mean value si engine model for control studies. In: *American Control Conference, 1990*. pp. 1882 –1887.

Hendricks, Elbert and Thomas Vesterholm (1992). The analysis of mean value si engine models. In: *SAE Technical Paper*. number 920682.

Imine, Hocine, Leonid Fridman, Hassan Shraim and Mohamed Djemai (2011). *Sliding mode based analysis and identification of vehicle dynamics*. Vol. 414. Springer Verlag.

Krstic, M., I. Kanellakopoulos and P. Kokotovic (1995). *Nolinear and Adaptive Control Design*. Wiley-Interscience. New York.

Levant., Arie (2003). Higher-order sliding modes, differentiation and output-feedback control. *International Journal of Control* **76**(9-10), 924–941.

Loukianov, A.G. (1998). Nonlinear block control with sliding mode. *Automation and Remote Control* **59**(7), 916–933.

Loukianov, A.G., S.J. Dodds, W. Hosny and J. Vittek (1997). A robust automotive controller design. In: *Control Applications, 1997., Proceedings of the 1997 IEEE International Conference on*. pp. 806 –811.

Moskwa, John J. and J. Karl Hedrick (1987). Automotive engine modeling for real time control application. In: *American Control Conference, 1987*. pp. 341 –346.

Rajamani, Rajesh (2012). *Vehicle Dynamics and Control*. Springer.

Shraim, Hassan, Mustapha Ouladsine, Leonid Fridman and Monica Romero (2008). Vehicle parameter estimation and stability enhancement using sliding modes techniques. *International Journal of Vehicle Design* **48**(3), 230–254.

Utkin, V.I. (1993). Sliding mode control design principles and applications to electric drives. *Industrial Electronics, IEEE Transactions on* **40**(1), 23–36.